

# Fiber-Optic Measurement Systems: Microwave and Radio Frequency Heating Applications

**Juming Tang**

*Department of Biological Systems Engineering, Washington State University, P. O. Box 646120, Pullman, Washington 99164-6120, U.S.A.*

## Abstract

Fiber-optic sensors do not interfere with electromagnetic fields and are commonly used to measure temperature and pressure used in microwave and frequency heating research and applications. This article introduces the physical principles for three different types of commonly used fiber-optic sensors and discusses important parameters to be considered in selecting appropriate fiber-optic sensors for rapid heating applications.

## INTRODUCTION

Temperature measurements are necessary for the development and control of dielectric heating processes in food and agricultural processing applications, such as drying, cooking, thawing, cooking, pasteurization, and sterilization. Conventional temperature sensors based on thermoelectric effects (e.g., thermocouples, RTD, and thermistors) distort the electromagnetic field in the vicinity of the probes and give erroneous readings. Fiber-optic sensors, on the other hand, do not interact with electromagnetic energy. They are now commonly used in microwave and radio frequency heating research and industrial operations.

Fiber-optic temperature sensors provide comparable accuracy to thermocouples in a normal heating medium. The probe sizes of fiber-optic sensors are generally small. For example, Luxtron Corporation (Santa Clara, CA) produces a standard fiber-optic temperature sensor with an outer diameter as small as 0.5 mm and FISO Technologies, Inc. (Quebec, QC, Canada) supplies sensors as small as 0.3 mm diameter. The response times of commercial fiber-optic temperature sensors in liquid media vary between 0.05 and 2 s, which make them well-suited for measuring relatively rapid temperature rises in materials during microwave or radio frequency (RF) heating. Fiber-optic sensors have been used extensively in research to monitor temperature and pressure changes during high temperature short-time microwave and RF drying and sterilization processes.<sup>[1–4]</sup>

*Keywords:* Temperature; Pressure; Sensor; Microwave; Radio frequency; Heating; Pasteurization; Sterilization; Response time; Thermal lag.

## PRINCIPLE OF FIBER-OPTIC TEMPERATURE SENSORS

Fiber-optic temperature sensors are developed based on one of three methods: fluorescence decay time, Fabry–Pérot interferometry, and transmission spectrum shift in semiconductor crystals. The physical principles used for the design of those systems vary from companies to companies.

### Fluorescence Decay Time

This technique is used by Luxtron Corporation (Santa Clara, CA)<sup>[5]</sup> and Ipitek (Carlsbad, CA). Luxtron, founded in 1978, commercializes its fiber-optic temperature sensors under the registered trademark Fluoroptic Technology. Their products were developed based on a unique optical property of phosphorescent materials, a.k.a. phosphors: the decay time of the sensor's emitted light varies precisely with temperature.

Fluoroptic technology uses a fiber-optic cable to connect the sensor to the instrument. In Luxtron's temperature sensors, a phosphor element is attached to the tip of a silica fiber and encapsulated in Teflon<sup>®</sup> tube. The phosphor material was excited with a light source. Early generation Fluoroptic thermometry systems used xenon flash lamps as the light sources, but current systems use smaller and more reliable light-emitting diodes (LEDs). In operation, the instrument sends pulses of light from the LED through the fiber to the sensor. The light pulses excite the phosphorescent sensor causing it to emit light.

The Luxtron sensor emits radiation over a broad spectrum in the near infrared region (Fig. 1). The emitted light returns to the Luxtron instrument through the same fiber-optic cable. Because the excitation light and emitted

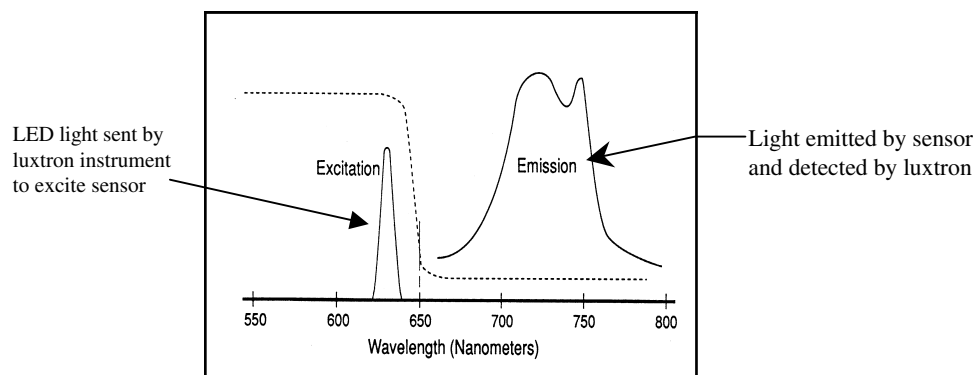


**Fig. 1** Spectral excitation and emission from Luxtron's Fluoroptic sensor. (Courtesy of Luxtron.)

light are of different colors, the instrument can distinguish between the two signals.

After the LED is turned off, the decaying fluorescent signal (Fig. 2) continues to transmit through the fiber to the instrument, where it is focused onto a detector.

The rate of the afterglow decay is dependent on the phosphor temperature. In general, the colder the sensor, the longer the decay time of the phosphor's emitted light. The measured decay time is then converted to the temperature of the phosphor (Fig. 3) using a built-in conversion table. Different conversion tables are used depending on temperature range and application. The overall temperature range capability of current technology is between  $-200$  and  $330^{\circ}\text{C}$ , typically to a precision of  $0.1^{\circ}\text{C}$ – $0.2^{\circ}\text{C}$ . The accuracy of calibrated temperature sensors is in the order of  $\pm 0.5^{\circ}\text{C}$ .

The fact that the excitation light signal and the fluorescent decay signal share the same optic cable makes it possible to produce small-diameter probes. This is particularly important in applications where there is a need to minimize disturbance to the object being measured.

A special application of Fluoroptic technology is measuring the surface temperature of fast moving objects

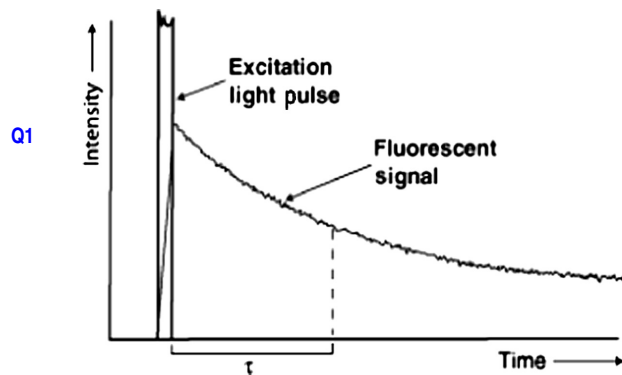


**Fig. 2** Decay of after-glow emitted by a phosphor sensor. (Courtesy of Luxtron.)

with a non-contact sensing method. Luxtron's remote sensor kit provides users with supplies and instructions to paint a small patch of the sensor material onto the object to be measured (Fig. 4). Once applied, the sensor can be observed remotely using an optical probe. This method offers the advantages of short response time and nonperturbation of the measured object.

### Fabry–Pérot Interferometry

FISO Technologies (Quebec, QC, Canada) and Photonics (Peabody, MA, U.S.A., ceased to operate in 2002) developed their temperature and pressure sensors based on an interferometer, otherwise referred to as white light interferometry (WLI). The sensing element of the probe based on WLI is a Fabry–Pérot interferometer (FPI), which is permanently attached to the tip of an optical fiber. The FPI interferometer consists of two parallel reflective surfaces (mirrors) attached to each end. These two reflective mirrors face each other and form a cavity resonator. FISO's FPI-based sensors use a thermally expandable piece of glass between the two reflected surfaces. The length of this piece defines the FPI cavity

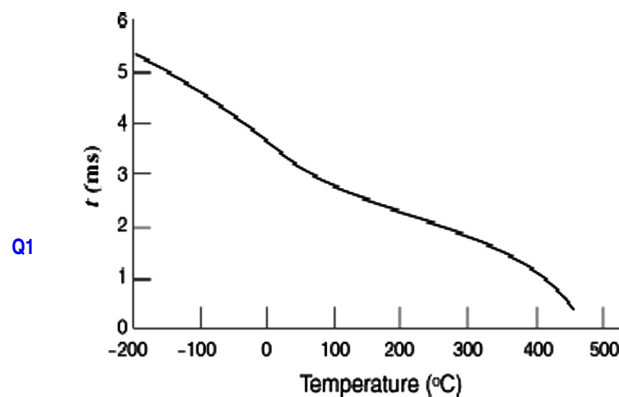


**Fig. 3** The decay time of phosphor afterglow (time to decay to  $1/e$  of the original strength) according to temperature. (Courtesy of Luxtron.)

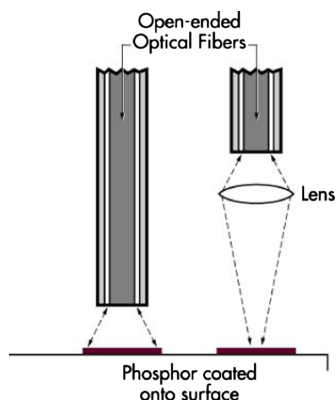


Fig. 4 Schematic drawing of Luxtron's remote sensing method. (Courtesy of Luxtron.)

depth (1–2 wavelengths deep) and changes with temperature due to thermal expansion. The measurement of other physical parameters, such as pressure, is also possible when using FPI interferometry. Fiber-optic pressure sensors can be very useful in studying the influence of internal pressure on texture and drying rate during microwave and RF drying operations.<sup>1</sup>

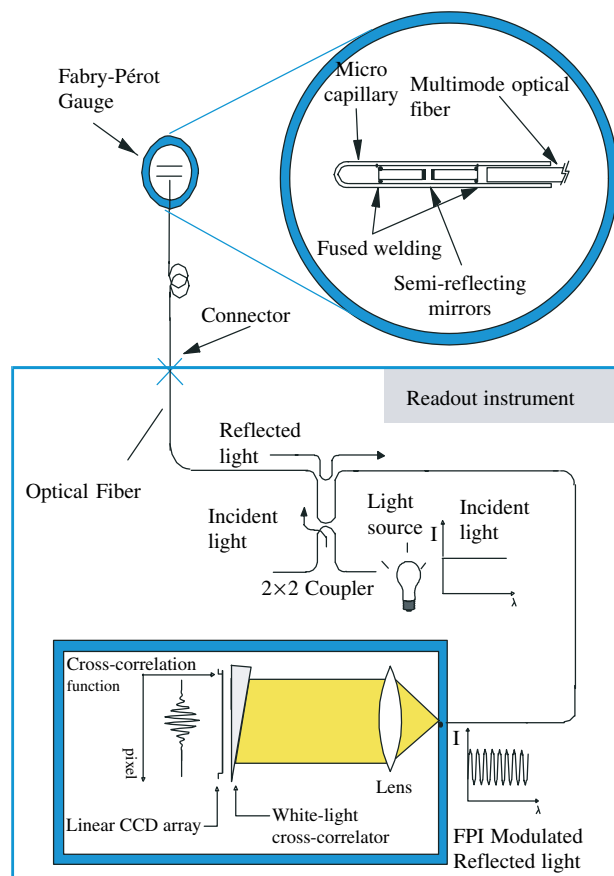


Fig. 5 Schematics showing the principles of FPI for the FISO system. (Courtesy of FISO Technologies, Inc.)

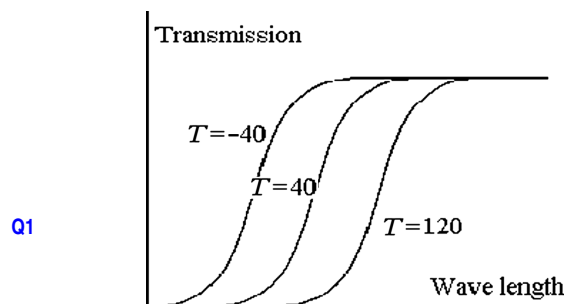


Fig. 6 Transmission spectrum shift in semiconductor crystals.

Cavity length in FPI sensors changes in response to strains, external stresses, or temperature changes. The key to the successful use of FPI technology depends on an effective means of obtaining precise and reliable Fabry–Pérot cavity length measurements. In the FISO systems, a white-light cross-correlator is used to measure the FPI cavity length. In principle, white light from a broadband source is directed into one arm of a 2×2 coupler and directed toward the Fabry–Pérot gauge (Fig. 5). The wavelength of the light is modulated by the gauge (FPI cavity) and reflected back toward the sensor readout instrument. The wavelength-modulated light is transmitted through a white-light cross-correlator and detected by a linear charge-coupled device (CCD) array. The white-light cross-correlator acts as a spatially distributed Fabry–Pérot cavity in which the cavity length varies along the lateral position. Interaction of the modulated light and the correlator generates a light pattern detected by the CCD array to yield information on the length of the FPI cavity. When used in microwave or RF processes, changes in the FPI cavity path or in the optical path length of the resonators are measured to determine the temperature or pressure experienced by the sensing element through a pre-established relationship between FPI cavity length and measured physical parameters Cable and Saaski.<sup>16]</sup>

### Transmission Spectrum Shift in Semiconductor Crystal

In the early nineties, Nortech-Fibronic Inc. (Quebec, QC, Canada) developed their temperature measurement sensors using the temperature-dependent light absorption/transmission characteristics of a semiconductor crystal gallium arsenide (or GaAs). A unique feature of this crystal is that when temperature increases, the crystal's transmission spectrum shifts to a higher wavelength (Fig. 6). Measuring the position of the absorption shift, using a grating-based near infrared spectrometer, provides information on the temperature of the sensing element.

Specifically, the Nortech sensors consist of a multi-mode optical fiber packaged in two layers of durable PTFE Teflon, terminated in a semiconductor (GaAs) crystal and a dielectric mirror at the fiber tip (Fig. 7). A beam of

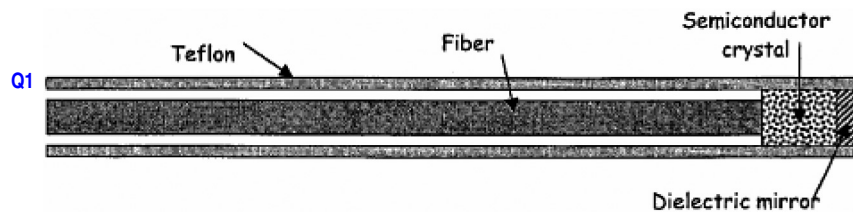


Fig. 7 Schematic diagram of a GaAs probe. (Courtesy of Neoptix Inc.)

multi-wavelength light is emitted from the light source in the signal conditioner and travels through a 2×1 optical coupler towards the sensor. Changes in the temperature of the GaAs crystal alter the transmission spectrum. The transmitted light through the semiconductor crystal impinges on the mirror at the end of the sensor, and is reflected back to the spectrum analyzer via the optical coupler. This optical signal is then converted into an electrical signal using a CCD. The electronics in the readout device evaluate the cutoff wavelength of absorption within the multi-wavelength spectrum. Analysis of the optical spectrum detected by the spectrum analyzer provides the crystal's temperature.

Nortech-Fibronic ceased to provide temperature sensors in 2001, FISO acquired the rights to manufacture and sell these sensors in 2001, and Neoptix acquired similar rights in 2004. The temperature calculation in the instrument depends solely on the wavelength of the transition of a fundamental physical characteristic of the GaAs. These systems are, therefore, immune to signal intensity, thus making it possible to develop probes up to 1,000 m. This technology also eliminates the need to enter a gage factor when interchanging probes. The typical response time of the Neoptix probes in water is 0.25 s and probes can be as small as 0.4 mm.

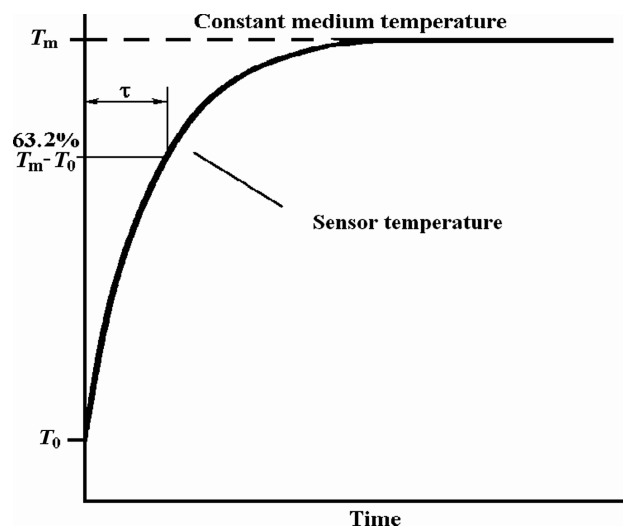


Fig. 8 Definition of response time,  $\tau$ , of a temperature sensor.

### APPLICATION CONSIDERATIONS

Fiber-optic sensors are often used for temperature measurement in ambient environments and not specifically designed for high temperature measurement in a pressurized environment. Careful selection of types of protection sleeves for fiber-optic sensors are necessary to ensure that the sensors can endure the hostile high temperature and pressure in thermal processing environment. Fiber-optic sensors are generally very fragile and require regular calibration to ensure that temperature readings are reliable.

Microwave and RF heating are rapid. It is, therefore, critical that the response time of the sensors,  $\tau$ , is small enough to accurately follow the rapid temperature changes in microwave and RF heating applications (see definition in Fig. 8). A large thermal lag in the temperature sensors used in process control would significantly underestimate the product temperature during rapid heating processes (Fig. 9). The following relationship can be used to assess if a temperature sensor has an adequately short response time for a rapid heating process, assuming a linear ramping temperature change:

$$\tau = \Delta T / \dot{T} \tag{1}$$

where  $\tau$  is the thermal response time of the sensor in the measured product, the time needed for the sensor to reach

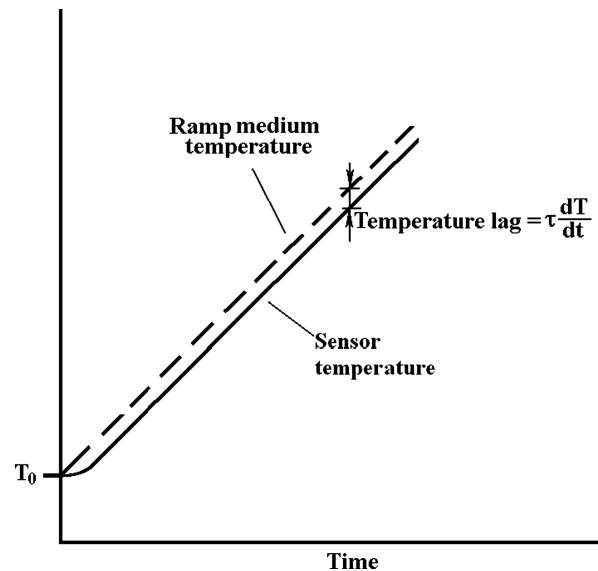


Fig. 9 Temperature lag of a sensor when subjected to a linear temperature ramp in the test medium.

63.2% of a step-change in medium temperature  $\Delta T$  is maximum allowable temperature lag, and  $\dot{T}$  (or  $dT/dt$ ) is heating rate.

For example, thermal processes to produce shelf-stable low acid foods are among the most regulated food processing operations that demand accurate temperature measurements for process development and control. In those applications, it is required that temperature measurement errors be less than 0.5°C. In the microwave-based thermal processes reported by Ohlsson<sup>[7]</sup> and Guan et al.,<sup>[2]</sup> the heating rate was 1 and 0.33°C/s, respectively. Based on Eq. 1, the response time of the temperature sensors should be less than 0.5 and 1.67 s, respectively, in order to limit the measurement error due to thermal lag to less than 0.5°C. It is possible that even more rapid microwave heating processes are used in the food industry, which would require shorter response times. Not all fiber-optic sensors can satisfy this requirement. For applications that involve microwave or RF heating in conjunction with heating with pressurized water or steam, fiber-optic sensors from certain companies do not perform well. Users need to be very carefully in evaluating the performance of fiber-optic sensors and select appropriate sensors to meet the specific requirements of desired applications.

#### ACKNOWLEDGMENTS

The author acknowledges the following company representatives for reviewing the article and providing relevant information and comments: Maryse Imbeault and Luc Langlois of FISO Technologies (500 St-Jean-Baptiste,

Ave, Suite 195, Quebec City, Quebec, Canada), Michel Plourde of Neoptix, Inc. (1415 Charest Quest Blvd, Suite 220, Quebec City, Quebec, Canada), William R. Kolbeck and Lenny Shaver of Luxtron (3033 Scott Blvd, Santa Clara, CA, U.S.A.), and Denis-Luc Charbonneau of Ipiteck (2330 Faraday Avenue, Carlsbad, CA, U.S.A.).

#### REFERENCES

1. Feng, H.; Tang, J.; Cavalieri, R.P.; Plumb, O.A. Heat and mass transport in microwave drying of hygroscopic porous materials in a spouted bed. *AICHE. J.* **2001**, *74* (7), 1499–1511.
2. Guan, D.; Plotka, V.C.F.; Clark, S.; Tang, J. Sensory evaluation of microwave treated macaroni and cheese. *J. Food Process. Preserv.* **2002**, *26*, 307–322.
3. Wang, Y.; Wig, T.; Tang, J.; Hallberg, L.M. Sterilization of foodstuffs using radio frequency heating. *J. Food Sci.* **2003**, *68* (2), 539–544.
4. Luechapattanaporn, K.; Wang, Y.; Wang, J.; Tang, J.; Hallberg, L.M. Microbial safety in radio frequency processing of packaged foods. *J. Food Sci.* **2004**, *67* (7), M201–M206.
5. Berek, H.E.; Wickersheim, K.A. Measuring temperatures in microwaveable packages. *J. Packaging Technol.* **1988**, 164–168.
6. Cable, D.W.; Saaski, E. Fiber-optic pressure measurement of spontaneous bumping/splattering of foods during microwaving. *Food Technol.* **1990**, *44* (6), 120.
7. Ohlsson, T. Sterilization of food by microwaves. SIK (the Swedish Institute for Food and Biotechnology). Report No. 564. Presented at the International Seminar on New Trends in Aseptic Processing and Packaging of Foodstuffs. Munich, 1987, Oct. 22–23.

**Author Queries**

*JOB NUMBER:* EOAF 120041609/217722

*TITLE:* Fiber-Optic Measurement Systems: Microwave and Radio Frequency Heating Applications

Q1 Please check the quality of figures.

561  
562  
563  
564  
565  
566  
567  
568  
569  
570  
571  
572  
573  
574  
575  
576  
577  
578  
579  
580  
581  
582  
583  
584  
585  
586  
587  
588  
589  
590  
591  
592  
593  
594  
595  
596  
597  
598  
599  
600  
601  
602  
603  
604  
605  
606  
607  
608  
609  
610  
611  
612  
613  
614  
615  
616

617  
618  
619  
620  
621  
622  
623  
624  
625  
626  
627  
628  
629  
630  
631  
632  
633  
634  
635  
636  
637  
638  
639  
640  
641  
642  
643  
644  
645  
646  
647  
648  
649  
650  
651  
652  
653  
654  
655  
656  
657  
658  
659  
660  
661  
662  
663  
664  
665  
666  
667  
668  
669  
670  
671  
672